

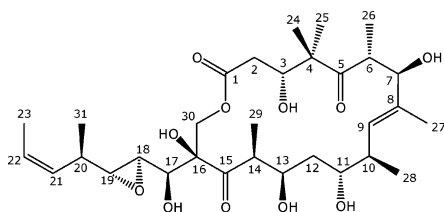
## Tedanolide C: A Potent New 18-Membered-Ring Cytotoxic Macrolide Isolated from the Papua New Guinea Marine Sponge *Ircinia* sp.

Camille Chevallier,<sup>†</sup> Tim S. Bugni,<sup>†</sup> Xidong Feng,<sup>‡</sup>  
Mary Kay Harper,<sup>†</sup> Anita M. Orendt,<sup>§</sup> and  
Chris M. Ireland<sup>\*,†</sup>

Department of Medicinal Chemistry, University of Utah, Salt Lake City, Utah 84112, Wyeth Research, Pearl River, New York 10965, and Center for High Performance Computing, University of Utah, Salt Lake City, Utah 84112

cireland@pharm.utah.edu

Received November 3, 2005



Tedanolide C (**1**)

Cytotoxicity-guided fractionation of the crude methanol extract of a marine sponge, *Ircinia* sp., yielded tedanolide C (**1**), a new 18-membered macrolide. The structure was solved by interpreting NMR and MS data, and the relative stereochemistry was determined from a combination of homo- and heteronuclear coupling constants in conjunction with molecular modeling. Compound **1** exhibited potent cytotoxicity against HCT-116 cells in vitro. Cell cycle analysis showed that treatment of cells with compound **1** arrested cells in the S-phase.

The promising bioactivity and the structural diversity within the marine environment continue to yield new secondary metabolites.<sup>1</sup> The encouraging current number of marine natural products and related compounds in clinical and advanced preclinical trials is evidence that marine secondary metabolites are important sources of new drugs.<sup>2</sup> As part of our natural products screening program for new anticancer lead compounds,<sup>3</sup> the extract of the marine sponge, *Ircinia* sp. collected in Milne Bay, Papua New Guinea, was shown to be very active in cytotoxicity assays against an HCT-116 cell line. Cytotoxicity-guided fractionation of the extract yielded (**1**), a new highly potent 18-membered macrolide. Over the past few years, several classes of macrolides have been isolated from marine sponges.

\* To whom correspondence should be addressed. Tel: 801-581-8305. Fax: 801-585-6208.

<sup>†</sup> Department of Medicinal Chemistry, University of Utah.

<sup>‡</sup> Wyeth Research.

<sup>§</sup> Center for High Performance Computing, University of Utah.

(1) Blunt, J. W.; Copp, B. R.; Munro, M. H. G.; Northcote, P. T.; Prinsep, M. R. *Nat. Prod. Rep.* **2004**, *21*, 1–49.

(2) Newman, D. J.; Cragg, G. M. *J. Nat. Prod.* **2004**, *67*, 1216–1238.

These include two closely related 18-membered macrolides, tedanolide (**2**)<sup>4</sup> and 13-deoxytedanolide (**3**)<sup>5</sup> from *Tedania ignis* and *Mycale adhaerens*, respectively, laulimalide,<sup>6</sup> a 20-membered ring from *Cacospongia mycofijiensis*, *Hyatella* sp., *Fasciospongia* sp., *Dactylospongia* sp., and also from a chromodorid nudibranch, and peloruside A,<sup>7</sup> a 16-membered ring macrolide from *Mycale hentscheli*. Tedanolide C (**1**) has the same macrolide ring size as tedanolide and 13-deoxytedanolide but a different oxygenation and methylation pattern. Herein, we report the isolation, the structure elucidation, the relative stereochemistry, cytotoxic evaluation of tedanolide C (**1**), and its activity on the cell cycle progression of HCT-116 cells.

The specimen of *Ircinia* collected from Papua New Guinea was extracted with MeOH. The crude extract was subjected to a solvent partition scheme to yield hexane, CHCl<sub>3</sub>, and aqueous MeOH extracts. The CHCl<sub>3</sub> extract was subjected to reversed-phase flash column chromatography using a MeOH/H<sub>2</sub>O gradient. The fraction eluting with 50:50 MeOH/H<sub>2</sub>O was concentrated to provide 145.4 mg of material that was further separated by HPLC using a reversed-phase semipreparative column to provide 15.7 mg of tedanolide C (**1**) (0.003% wet weight).

Compound **1** was obtained as a white amorphous solid. The HRESIMS gave an [M + Na]<sup>+</sup> ion at *m/z* 621.3242 (calcd 621.3250) corresponding to the formula C<sub>31</sub>H<sub>50</sub>O<sub>11</sub>Na<sup>+</sup>, which was consistent with both the <sup>1</sup>H and <sup>13</sup>C NMR spectra. The IR spectrum contained absorption bands for hydroxyl, ester, and ketone groups (3418, 1736, 1697 cm<sup>-1</sup>). <sup>13</sup>C and DEPT experiments confirmed the presence of 31 carbons, which were distributed as 6 quaternary, 14 methine, 3 methylene, and 8 methyl carbon atoms. Additionally, these spectra revealed the presence of two saturated ketone carbonyls, one ester carbonyl, one quaternary olefin carbon, three protonated olefinic carbons, seven oxymethine carbons, and one quaternary oxygenated carbon. This carbon inventory explained five of the seven degrees of unsaturation, indicating **1** is bicyclic. The <sup>1</sup>H NMR spectrum revealed three downfield olefinic protons, seven downfield oxymethine protons, three methylene groups, four upfield methine protons attached to carbons bearing methyls, four corresponding aliphatic secondary methyl groups (doublets), two upfield tertiary methyl groups (singlets) and two vinyl methyls (one singlet, one doublet) (see Table 1). Cross-peaks in the COSY spectrum indicated five continuous spin systems. Thereafter, these data along with HSQC, HSQC-TOCSY, and

(3) Ireland, C. M.; Aalbersberg, W.; Andersen, R. J.; Ayral-Kaloustian, S.; Berlinck, R.; Bernan, V.; Carter, G.; Churchill, A. C. L.; Clardy, J.; Concepcion, G. P.; Dilip De Silva, E.; Discifani, C.; Fojo, T.; Frost, P.; Gibson, D.; Greenberger, L. M.; Greenstein, M.; Harper, M. K.; Mallon, R.; Loganzo, F.; Nunes, M.; Poruchynsky, M. S.; Zask, A. *Pharm. Biol.* **2003**, supplement 1, *41*, 15–38.

(4) Schmitz, F. J.; Gunasekera, S. P.; Yalamanchili, G.; Bilayet Hossain, M.; Van Der Helm, D. *J. Am. Chem. Soc.* **1984**, *106*, 7251–7252.

(5) Fusetani, N.; Sugawara, T.; Matsunaga, S.; Hirota, H. *J. Org. Chem.* **1991**, *56*, 4971–4974.

(6) (a) Corley, D. G.; Herb, R.; Moore, R. E.; Scheuer, P. J. *J. Org. Chem.* **1988**, *53*, 3644–3646. (b) Jefford, C. W.; Bernadinelli, G.; Tanaka, J.; Higa, T. *Tetrahedron Lett.* **1996**, *37*, 159–162. (c) Mooberry, S. L.; Tien, G.; Hernandez, A. H.; Plubrukarn, A.; Davidson, B. S. *Cancer Res.* **1999**, *59*, 653–660.

(7) (a) West, L. M.; Northcote, P. T.; Battershill, C. N. *J. Org. Chem.* **2000**, *65*, 445–449. (b) Hood, K. A.; West, L. M.; Rouwé, B.; Northcote, P. T.; Berridge, M. V.; Wakefield, St. J.; Miller, J. H. *Cancer Res.* **2002**, *62*, 3356–3360.

TABLE 1. NMR Data for Tedanolide C (1) (CD<sub>3</sub>OD)<sup>a</sup>

pos	$\delta_C$ multiplicity	$\delta_H$ multiplicity (Hz)	COSY	HMBC	NOESY	HETLOC, HSQMBC (Hz) <sup>b</sup>
1	172.6 s					
2	39.3 t	2.17 dd, 14.6, 11.2	2a, 3	1,3	3	3 (-6.0)
		2.26 dd, 14.6, 2.8	2b, 3		3	3 (-2.0)
3	73.1 d	4.14 dd, 11.2, 2.8	2a, 2b	2, 4, 24, 25	2a, 2b, 14, 24	
4	53.2 s					
5	220.5 s					
6	46.9 d	3.21 dq, 9.2, 7.2	7, 26	5, 7, 8, 26	7, 24, 27	7 (-4.6)
7	81.3 d	4.06 d, 9.2	6	6, 26, 27	6	6 (3.3), 26 (3.3)
8	136.0 s					
9	134.1 d	5.18 d, 9.2	10	7, 10, 11, 27	11, 12a, 28	11 (3.3)
10	40.4 d	2.20 ddq, 9.2, 6.9, <1.0	9, 11, 28	8, 9, 11, 28	28	11 (5.5)
11	73.8 d	3.53 dd, 10.3, 2.9	10, 12b	10, 13, 28	9, 12a, 28	13 (3.6), 28 (3.2)
12	41.5 t	1.15 ddd, 15.3, 10.3, 3.6	11, 12a		12a, 14	11 (-5.5), 13 (1.2), 14 (5.5),
		1.40 ddd, 15.3, 9.9, 2.9	12b, 13		9, 11, 12b, 13, 14	11 (-1.1), 13 (-5.8), 14 (0)
13	70.2 d	4.05 ddd, 9.9, 3.6, 3.3	12a		12a	11 (3.3), 29 (3.3)
14	48.9 d	3.31 dq, 7.2, 3.3	29	12, 13, 15, 29, 30	3, 12a, 12b, 29	13 (-2.8), 15 (4.0)
15	219.7 s					
16	84.5 s					
17	75.1 d	3.51 d, 7.4	18	15, 16, 18, 19	18, 19, 30a, 30b	15 (1.7), 16 (2.0), 18 (4.0)
18	59.1 d	2.99 dd, 7.4, 2.0	17, 19	17, 19, 20	17, 19, 20, 23, 30a, 31	17 (4.5), 19 (1.3)
19	62.3 d	2.74 dd, 6.9, 2.0	18, 20	17, 18, 20, 21, 23, 31	17, 18, 20, 21, 30a, 30b, 31	17 (2.0), 18 (1.3), 20 (6.3),
						21 (1.3), 31 (2.6)
20	35.3 d	2.41 ddq, 10.3, 6.9, 6.9	19, 21, 31	18, 19, 21, 22, 23, 31	18, 19, 23, 31	19 (-7.0)
21	131.6 d	5.27 ddq, 10.8, 10.3, 1.6	20, 22, 23	19, 20, 23, 31	19, 22, 31	
22	127.1 d	5.54 dq, 10.8, 6.8	21, 23	20, 23	21, 23	
23	13.5 q	1.61 dd, 6.8, 1.6	21, 22	19, 20, 21, 22	18, 20, 22	
24	25.0 q	1.16 s		3, 4, 5, 25	3, 6	
25	18.7 q	1.22 s		3, 4, 24		
26	17.6 q	1.21 d, 7.2	6	5, 6, 7		
27	11.3 q	1.54 s		7, 8, 9	6, 28	
28	17.7 q	0.97 d, 6.8	10	9, 10, 11	9, 10, 11, 27	
29	12.6 q	1.21 d, 7.2	14	14, 15	14	
30	70.3 t	4.02 d, 11.0	30a	1, 15, 16	17, 19, 30a	15 (1.5)
		4.18 d, 11.0	30b		17, 18, 19, 30b	15 (5.5), 16 (5.0)
31	18.0 q	1.06 d, 6.9	20	19, 20, 21	18, 19, 20, 21	

<sup>a</sup> Data obtained on a 400 MHz instrument. <sup>b</sup> Data obtained on a 500 MHz instrument. Signs for the  $^2J_{CH}$  coupling constants measured from the HSQMBC experiments are not mentioned.

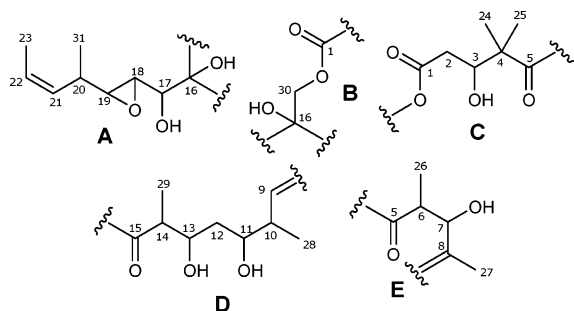


FIGURE 1. Partial structures A–E determined for tedanolide C (1).

HMBC data allowed assignments of the five partial structures shown in Figure 1.

For partial structure A,  $^1H$  and  $^{13}C$  chemical shifts indicated the presence of one *Z* double bond ( $J_{21,22} = 10.8$  Hz) between C-21 [ $\delta_H$  5.27;  $\delta_C$  131.6] and C-22 [ $\delta_H$  5.54;  $\delta_C$  127.1]. C-17 was oxygenated as judged by chemical shifts [ $\delta_H$  3.51;  $\delta_C$  75.1]. The methine proton H-20 showed an HMBC correlation with the methyl carbon C-31 [ $\delta$  18.0]. On the basis of  $^1H$  and  $^{13}C$  chemical shift data, C-19 [ $\delta_H$  2.74;  $\delta_C$  62.3] and C-18 [ $\delta_H$  2.99;  $\delta_C$  59.1] was part of a *trans* ( $J_{18,19} = 2.0$  Hz) epoxide and was confirmed by comparison with data from tedanolide<sup>4</sup> and 13-deoxytedanolide.<sup>5</sup> An HMBC correlation between the methine proton H-17 [ $\delta$  3.51] and the oxygenated carbon C-16 [ $\delta$  84.5] established the last connection for the remaining portion of the partial structure A. Partial structures D and E were established

by interpretation of COSY and HMBC spectra. The contiguous nature of C-9 through C-14 in partial structure D was easily assigned from the COSY spectrum. C-11 and C-13 were oxygenated, based on their  $^{13}C$  chemical shifts,  $\delta$  73.8 and 70.2, respectively. The  $^1H$  and  $^{13}C$  chemical shifts of C-9 [ $\delta_H$  5.18;  $\delta_C$  134.1] indicated it was part of a trisubstituted double bond. NOE correlations between the methyl group H<sub>3</sub>-27 and the proton H-10 showed that the C-8-C-9 double bond was in the *E* configuration. Partial structure E shared a characteristic COSY pattern for the sequence CH(CH<sub>3</sub>)CH(OH). This piece was connected to C-8 by an HMBC correlation with H-6 and to C-5 by an HMBC correlation from H-6.

Partial structure C was deduced by a combination of COSY and HMBC data. The COSY spectrum revealed the C-2-C-3 unit. A quaternary carbon at  $\delta$  53.2 showing HMBC correlations with H-3, H<sub>3</sub>-24, and H<sub>3</sub>-25 could be assigned as C-4.

The  $^1H$  shifts for H<sub>2</sub>-30 ( $\delta$  4.02, 4.18) indicated that these protons were an oxymethylene that displayed clear HMBC correlations to the ester carbonyl C-1 ( $\delta$  172.6) and to the quaternary oxygenated carbon C-16 ( $\delta$  84.5). Long-range proton coupling correlations from the oxymethine proton H-17 to carbons C-15, and C-16 and from methylenic proton H<sub>2</sub>-30 to ketone C-15 revealed the attachment points between C-15-C-16-C-30. The attachment point provided supportive evidence for the connection of partial structures A, B and D. Cross-peaks in the HMBC spectrum from H<sub>3</sub>-24 to C-5, H-6 to C-5 and from H<sub>3</sub>-26 to C-5 allowed connection of partial structures C

and E. Proton H<sub>2</sub>-2 showed an HMBC correlation to C-1, linking partial structures B and C.

Initially, we planned to establish the relative stereochemistry using the *J*-based configuration analysis<sup>8</sup> and DPGSE 1D NOE<sup>9</sup> experiments in conjunction with molecular modeling. Several limitations regarding compound **1** made it clear that we had to take an iterative approach that combined extensive molecular modeling studies with an extension<sup>10</sup> of *J*-based method followed by repetitive adjustments to the structure and finally DFT calculations on the intact molecule. Measurement of homonuclear coupling data was achieved utilizing <sup>1</sup>H and DQF-COSY experiments. Heteronuclear couplings were measured using a GHETLOC<sup>11</sup> and a G-BIRD<sub>R</sub>-HSQMBC.<sup>12</sup> A lowest energy conformer was first identified by molecular dynamics using AMBER.<sup>13</sup> Subsequently, GAUSSIAN<sup>14</sup> was used for geometry optimization (d95\*\* basis set, B3LYP density functional) of the system and computation of *J* values on the intact molecule (EPRII basis set, B3LYP density functional).<sup>15</sup> The complete approach we used to help elucidate the relative stereochemistry, as well as a detailed account of the Gaussian calculations and evaluation of basis sets using model compounds will be presented elsewhere.

The epoxide was the starting point for the assignment of the relative stereochemistry. The <sup>1</sup>J<sub>HH</sub> for H-18 and H-19, 2.0 Hz, is typical of a *trans*-substituted epoxide.<sup>16</sup> The coupling constant between H-19 and H-20 was large in **1** (6.9 Hz) and in tetanolide (9.4 Hz),<sup>4</sup> but the stereochemistry of C-20 could still be different between the two compounds. This large homonuclear coupling suggested an anti relationship in **1** between these two protons. Measurement of <sup>2</sup>J<sub>CH</sub> coupling constant of -7.0 Hz between H-20 and C-19 indicated that H-20 was gauche to the electronegative oxygen substituent at C-19. Two <sup>3</sup>J<sub>CH</sub> of 1.3 and 2.6 Hz between H-19 and C-21, and H-19 and

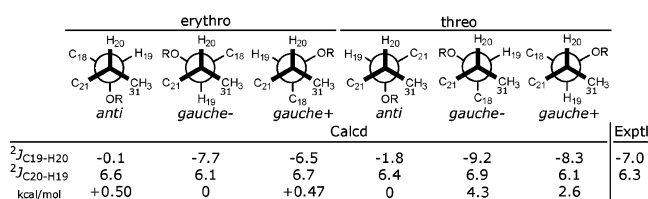


**FIGURE 2.** Energies, Newman projections, and comparison of experimental and calculated *J* values for the C-19–C-20 bond of **1**.

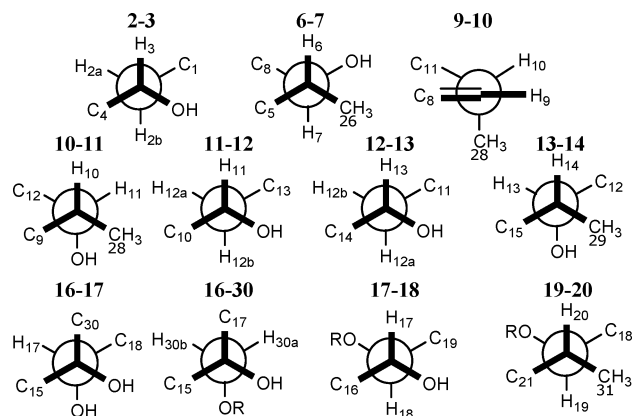


**FIGURE 3.** Diagram of the rotamers determined for the C–C bonds of tetanolide **C** (**1**).

C-31 respectively indicated that this proton was gauche to these two groups. A NOESY correlation was observed between H-20 and H-23. Only one rotamer (see Figure 3) fits all these data and thus represents the relative configuration of these two centers. *J* coupling values have been computed for each rotamer about the C-19–C-20 bond (see Figure 2). The calculated values (-7.7 and 6.1 Hz) for the erythro (-) gauche rotamer (<sup>13</sup>C-attached oxygen relative to the proton) showed the best correlation to the experimental data (-7.0 and 6.3 Hz respectively) for the C-19–C-20 bond of **1**, providing additional support for the assigned stereochemistry. Measured and calculated <sup>2</sup>J<sub>C20-H19</sub> are large, positive values with no angular dependence. Based on the energies (Figure 2), the Boltzmann distribution indicates that the threo system should be mostly in the anti conformation. This result clearly does not agree with our experimental data, especially the <sup>3</sup>J<sub>H19-H20</sub> and <sup>2</sup>J<sub>C19-H20</sub>.

For the C-17–C-18 bond, a large vicinal coupling constant between H-17 and H-18 (7.4 Hz) suggested that H-17 and H-18 were anti. A large two-bond C–H coupling constant measured for C-18/H-17 (4.0 Hz) suggested that H-17 was gauche to 18-OR. At this point the number of possible rotamers that would allow a large coupling constant between H-17 and H-18 is still two. From the calculated and measured vicinal <sup>1</sup>H coupling, there is no evidence of conformational averaging. A NOESY correlation was observed between H-17 and H-19. Thus, the relation between 17-OH and 18-OR was assigned as anti on the basis of these data.

(15) (a) Dunning, T. H.; Hay, P. J., Jr. In *Methods of Electronic Structure Theory*; Schaefer, H. F., III, Ed.; Plenum Press: New York, 1976; Vol. 3. (b) Becke, A. D. *J. Chem. Phys.* **1993**, *98*, 5648–5652. (c) Lee, C.; Yang, W.; Parr, R. G. *Phys. Rev. B* **1988**, *37*, 785–789. (d) Stevens, P. J.; Devlin, F. J.; Chabalowski, C. F.; Frisch, M. J. *J. Phys. Chem.* **1994**, *98*, 11623–11627. (e) Barone, V. In *Recent Advances in Density Functional Methods*; Chong, D. P., Ed.; World Scientific Publ. Co.: Singapore, 1996; Part I. (16) (a) Tsuda, M.; Sasaki, T.; Kobayashi, J. *J. Org. Chem.* **1994**, *59*, 3734–3737. (b) Shigemori, H.; Tanaka, Y.; Yazawa, K.; Mikami, Y.; Kobayashi, J. *Tetrahedron* **1996**, *52*, 9031–9034.

(8) Matsumori, N.; Kaneno, D.; Murata, M.; Nakamura, H.; Tachibana, K. *J. Org. Chem.* **1999**, *64*, 866–876.

(9) (a) Stott, K.; Stonehouse, J.; Keeler, J.; Hwang, T. L.; Shaka, A. J. *J. Am. Chem. Soc.* **1995**, *117*, 4199–4200. (b) Stott, K.; Keeler, J.; N. Van, Q.; Shaka, A. J. *J. Magn. Reson.* **1997**, *125*, 302–324.

(10) Williamson, R. T.; Marquez, B. L.; Barrios Sosa, A. C.; Koehn, F. E. *Magn. Reson. Chem.* **2003**, *41*, 379–385.

(11) Uhrin, D.; Batta, G.; Hruby, V. J.; Barlow, P. N.; Kover, K. E. *J. Magn. Reson.* **1998**, *130*, 155–161.

(12) (a) Williamson, R. T.; Marquez, B. L.; Gerwick, W. H.; Kover, K. E. *Magn. Reson. Chem.* **2000**, *38*, 265–273. (b) Marquez, B. L.; Gerwick, W. H.; Williamson, R. T. *Magn. Reson. Chem.* **2001**, *39*, 499–530. (c) Williamson, R. T.; Boulanger, A.; Vulpanovici, A.; Roberts, M. A.; Gerwick, W. H. *J. Org. Chem.* **2001**, *39*, 499–530.

(13) Case, D. A.; Darden, T. A.; Cheatham, T. E., III; Simmerling, C. L.; Wang, J.; Duke, R. E.; Luo, R.; Merz, K. M.; Wang, B.; Pearlman, D. A.; Crowley, M.; Brozell, S.; Tsui, V.; Gohlke, H.; Mongan, J.; Hornak, V.; Cui, G.; Beroza, P.; Schafmeister, C.; Caldwell, J. W.; Ross, W. S.; Kollman, P. A. *AMBER*.

(14) Frisch, M. J.; Trucks, G. W.; Schlegel, H. B.; Scuseria, G. E.; Robb, M. A.; Cheeseman, J. R.; Montgomery, J. A., Jr.; Vreven, T.; Kudin, K. N.; Burant, J. C.; Millam, J. M.; Iyengar, S. S.; Tomasi, J.; Barone, V.; Mennucci, B.; Cossi, M.; Scalmani, G.; Rega, N.; Petersson, G. A.; Nakatsuji, H.; Hada, M.; Ehara, M.; Toyota, K.; Fukuda, R.; Hasegawa, J.; Ishida, M.; Nakajima, T.; Honda, Y.; Kitao, O.; Nakai, H.; Klene, M.; Li, X.; Knox, J. E.; Hratchian, H. P.; Cross, J. B.; Bakken, V.; Adamo, C.; Jaramillo, J.; Gomperts, R.; Stratmann, R. E.; Yazyev, O.; Austin, A. J.; Cammi, R.; Pomelli, C.; Ochterski, J. W.; Ayala, P. Y.; Morokuma, K.; Voth, G. A.; Salvador, P.; Dannenberg, J. J.; Zakrzewski, V. G.; Dapprich, S.; Daniels, A. D.; Strain, M. C.; Farkas, O.; Malick, D. K.; Rabuck, A. D.; Raghavachari, K.; Foresman, J. B.; Ortiz, J. V.; Cui, Q.; Baboul, A. G.; Clifford, S.; Cioslowski, J.; Stefanov, B. B.; Liu, G.; Liashenko, A.; Piskorz, P.; Komaromi, I.; Martin, R. L.; Fox, D. J.; Keith, T.; Al-Laham, M. A.; Peng, C. Y.; Nanayakkara, A.; Challacombe, M.; Gill, P. M. W.; Johnson, B.; Chen, W.; Wong, M. W.; Gonzalez, C.; Pople, J. A. *Gaussian 03*, revision C.02; Gaussian, Inc.: Wallingford, CT, 2004.

The relative stereochemistry at position C-16 was established through the *J*-based analysis for C-16–C-17 and C-16–C-30 bonds. Measurement of a small  $^2J_{C16-H17}$  (2.0 Hz) and small  $^3J_{C15-H17}$  (1.7 Hz) coupling constants indicated that H-17 was anti to 16-OH and gauche to C-15. At this point, two rotamers satisfied these data. Molecular modeling was used to predict NOE patterns for each rotamer. One rotamer could be eliminated due to an observed NOE correlation between H-30a/H-18 which suggested a gauche orientation between these two protons. For the C-16–C-30 bond, a large  $^2J_{C16-H30a}$  (5.0 Hz), a large  $^3J_{C15-H30a}$  (5.5 Hz) and a small  $^3J_{C15-H30b}$  (1.5 Hz) heteronuclear couplings were measured, indicating that H-30a was gauche to 16-OH, anti to C-15 and that H-30b was gauche to C-15. NOE correlations between H-30a/H-17 and H-30b/H-17 finally established the relative stereochemistry depicted in Figure 3.

The relative orientation of H-9 and H-10 was demonstrated by a large homonuclear  $^3J_{H9-H10}$  (9.2 Hz) coupling constant, which suggested that these two protons should have an anti relationship and created confusion. However, a careful analysis of the best minimized molecular model revealed that the two protons were eclipsed. The two protons, H-9 and H-10, considered as eclipsed, indicated the relative stereochemistry depicted in Figure 3.

The rest of the stereocenters were also established using *J*-based analysis (see Figure 3). The relations between fragments were established through NOESY correlations analysis. NOESY correlations were observed for H-3/H-24, H-24/H-6, suggesting that H-3, H-6 and H-24 had gauche orientations. Similarly, fragments D and E (Figure 1) were related through an NOE correlation for H-6/H-27, H-27/H-28, and H-14/H-3. As explained above, for the determination of the relative stereochemistry at position C-16, fragments A, B and D (Figure 1) were related through the *J*-based analysis for C-16–C-17 and C-16–C-30 bonds and through observed NOESY correlations for H-30a/H-17 and H-30b/H-17 in conjunction with molecular modeling.

Compound **1** was tested against a colorectal cancer cell line (HCT-116, wild type) and displayed an  $IC_{50}$  of 0.057  $\mu\text{g/mL}$  ( $9.53 \times 10^{-8}$  M). Cell cycle analysis showed that treatment of HCT-116 cells with 0.2  $\mu\text{g/mL}$  of tedanolide C (**1**) resulted in a strong accumulation of cells in the S-phase after 24-h exposure and was sustained through 48-h exposure.

These potent results indicated that like 13-deoxytedanolide,<sup>17</sup> tedanolide C (**1**) could be an inhibitor of protein synthesis.

In conclusion, tedanolide C (**1**) is a new 18-membered macrolide isolated from the Papua New Guinea sponge *Ircinia* sp. This compound bears a different pattern of oxygenation and methylation when compared to tedanolide<sup>4</sup> and 13-deoxytedanolide.<sup>5</sup> The planar structure was established mainly by NMR methods. An extension of the *J*-based configuration analysis was applied successfully in conjunction with molecular modeling and DFT calculations to elucidate the relative stereochemistry of compound **1**. We have identified a method to extend the *J*-based method for conformers that present anti relationships between adjacent protons. Since the coupling constant pattern is identical for erythro and threo systems, normally the *J*-based method does not allow the stereochemical assignment. However, using the energies obtained from Gaussian for each possible rotamer from two diastereoisomers, one can use Boltzmann's equation to estimate the populations. Using this approach, we found that the threo diastereoisomer should be mostly in the (–) gauche conformation. This conformer clearly does not agree with the measured coupling values. Tedanolide C (**1**) exhibited potent cytotoxicity against HCT-116 cells in vitro with  $IC_{50}$  value

of  $9.53 \times 10^{-8}$  M and caused a strong S-phase arrest. A recent study of SARs of 13-deoxytedanolide<sup>5</sup> reported that the southern hemisphere comprised the pharmacophore, while the epoxide-bearing side chain was essential for the activity.<sup>18</sup> It has also been shown that 13-deoxytedanolide<sup>5</sup> is also a potent protein synthesis inhibitor and the first macrolide to inhibit the eukaryotic ribosome.<sup>17</sup> The study of the mechanism of action of compound **1**, as an S-phase arrest agent, is currently under investigation.

## Experimental Section

**Animal Material.** The specimen of *Ircinia* sp. was collected in Milne Bay (S 10° 14.278' E 150° 54.782'), Papua New Guinea, in 2001. A voucher specimen (PNG01-6-67) is held at the University of Utah.

**Extraction and Isolation.** Frozen sponge material (480 g) was extracted with MeOH (1 L) three times. The MeOH extracts were combined, filtered, and evaporated to dryness in vacuo to give a dark brown residue (16.5 g). This residue was dissolved in 10% water in MeOH (500 mL) and partitioned against hexane ( $3 \times 500$  mL). The water content of the MeOH phase was adjusted to 30% by adding 143 mL of water before partitioning against  $\text{CHCl}_3$  ( $3 \times 500$  mL). This solvent partition scheme yielded hexane (1.1 g),  $\text{CHCl}_3$  (1.8 g), and 30% aq MeOH (13.3 g) extracts. The  $\text{CHCl}_3$  extract was fractionated by C18 flash column chromatography using MeOH gradients in  $\text{H}_2\text{O}$ . The last fraction eluted with (50:50) MeOH/ $\text{H}_2\text{O}$  (145.4 mg) was further purified by phenyl hexyl HPLC using a  $\text{CH}_3\text{CN}/\text{H}_2\text{O}$  gradient (30:70 to 85:15 over 30 min) to afford tedanolide C (**1**, 15.7 mg).

**Tedanolide C (1):** white amorphous solid;  $[\alpha]_D^{24} + 21.4$  ( $c$  0.215; MeOH); UV (MeOH)  $\lambda_{\text{max}}$  ( $\epsilon$ ) 208 (8031) 264 (1096) nm; IR (film)  $\nu_{\text{max}}$  3418, 2972, 2933, 1736, 1697, 1457, 1372, 1294, 1253, 1169, 1076, 984, 903, 822, 756  $\text{cm}^{-1}$ ;  $^1\text{H}$  and  $^{13}\text{C}$  NMR data in Table 1; (+)-LRESIMS  $m/z$   $[\text{M} + \text{Na}]^+$  621.3; HRESIMS  $m/z$  621.32423 (calcd for  $\text{C}_{31}\text{H}_{50}\text{O}_{11}\text{Na}^+$ , 621.32508,  $\Delta$  –0.85 mmu).

**Acknowledgment.** This work was supported by NIH Grant No. CA36622. Funding for the Varian Inova 500 MHz NMR spectrometer was provided through NCI Grant No. 5 P30 CA 42014 and NIH Grant No. 1 S10RR06262. We acknowledge the government of Papua New Guinea for permits to collect the sponge and also Anna Senina and the HSC core facilities for performing the cell proliferation assay and the flow cytometry experiments, respectively. An allocation of computer time from the Center for High Performance Computing at the University of Utah is gratefully acknowledged. The computational resources for this project have been provided by the National Institutes of Health (Grant No. NCR1 S10 RR17214-01) on the Arches Metacluster, administered by the University of Utah Center for High Performance Computing. We thank Mr. Jay Olsen, University of Utah, for his assistance in acquiring NMR data.

**Note Added after ASAP Publication.** The relative energies of the anti and gauche (–) threo rotamers were switched in Figure 2 of the version published ASAP February 18, 2006; the corrected version was published February 21, 2006.

**Supporting Information Available:** Copies of  $^1\text{H}$ ,  $^{13}\text{C}$ , DQF-COSY, GHSQC, GHMBC, GHETLOC, and G-BIRD<sub>R</sub>-HSQMBC NMR data, general experimental procedures, fragmentation pathway for the  $[\text{M} + \text{Na}]^+$  ion observed in the ESI FTMS SORICID mass spectrum for **1**, biological assay descriptions, and three-dimensional structure of **1**. This material is available free of charge via the Internet at <http://pubs.acs.org>.

JO052285+

(17) Nishimura, S.; Matsunaga, S.; Yoshida, M.; Hirota, H.; Yokoyama, S.; Fusetani, N. *Bioorg. Med. Chem.* **2005**, *13*, 449–454.

(18) Nishimura, S.; Matsunaga, S.; Yoshida, S.; Nakao, Y.; Hirota, H.; Fusetani, N. *Bioorg. Med. Chem.* **2005**, *13*, 455–462.